DALTON
FULL PAPER

Solution and solid state structures of binuclear zinc(II) complexes of bis(pentadentate) ligands derived from bis(1,4,7-triazacyclononane) macrocycles

Suzanne J. Brudenell,[a] Leone Spiccia,*[a] David C. R. Hockless[b] and Edward R. T. Tiekink[c]

[a] *Department of Chemistry, Monash University, Clayton, Victoria, 3168, Australia*
[b] *Research School of Chemistry, Australian National University, Canberra, ACT, 2601, Australia*
[c] *Department of Chemistry, The University of Adelaide, Adelaide, South Australia, 5005, Australia*

Received 22nd December 1998, Accepted 1st March 1999

Binuclear zinc(II) complexes have been prepared for bis(pentadentate) ligands, generated by addition of 2-pyridylmethyl arms to the secondary nitrogens in bis(1,4,7-triazacyclononane) macrocycles, and supported by CH_2CH_2 {tmpdtne, $[Zn_2(tmpdtne)Br_2][ClO_4]_2\cdot H_2O$ **1**}, $CH_2CH_2CH_2$ {tmpdtnp, $[Zn_2(tmpdtnp)Br_2][ClO_4]_2\cdot 3H_2O$ **2**}, $CH_2CH_2CH_2CH_2$ {tmpdtnb, $[Zn_2(tmpdtnb)][ClO_4]_4\cdot 3DMSO$ **3**}, *m*-$CH_2C_6H_4CH_2$ {tmpdtn*m*-X, $[Zn_2(tmpdtnm\text{-}X)][ClO_4]_4$ **4**} and $CH_2CH(OH)CH_2$ {tmpdtnp-OH, $[Zn_2(tmpdtnp\text{-}O)][ClO_4]_3$ **5**} backbones. The crystal structure of **5** confirmed that the two zinc(II) centres are linked by an endogenous alkoxo bridge generated by deprotonation of the $CH_2CH(OH)CH_2$ backbone. A short intramolecular Zn · · · Zn separation of 3.904(2) Å is observed, which matches that found at the active site of alkaline phosphatase. For **1** a binuclear complex with Zn · · · Zn separation of 6.545(9) Å is formed. The distorted octahedral geometry about each zinc(II) centre is defined by five N-donors from the ligand and a bromide in the sixth position. The *transoid* angles involving one of the tacn nitrogens and either the bromide or a pyridyl nitrogen (148–169°) highlight the degree of distortion. The arrangement of donor atoms within the distorted octahedral co-ordination sphere of Zn^{II} is asymmetric with the bromide ligand *cis* to the bridgehead nitrogen. The series of zinc complexes display interesting variations in their solid state and solution stereochemistries. The ^1H NMR spectrum recorded at 300 K is broad indicating rearrangement between different structures on the NMR timescale. The signals become sharper at higher temperatures but only half the number expected from the solid state structure are observed. A rearrangement to a geometry (square pyramidal through loss of the halide ligand) that preserves the symmetry of the ligand occurs at higher temperatures. Compound **2** exhibits similar solution behaviour while for **3** and **4** the ^1H NMR spectra indicate that the symmetric disposition of the ligand is adopted even at room temperature. A correlation exists between the type of bridge linking the pentadentate compartments of the ligands and the preferred solution structure.

Introduction

Interest in the structure and reactivity of macrocyclic zinc(II) complexes has been growing in recent years. One of the driving forces for these studies is the presence of one or more zinc centres at the active sites of enzymes which catalyse hydration reactions (carbon dioxide), condensation reactions involved in the polymerization of RNA and a variety of hydrolytic processes involved in the cleavage of peptides, proteins and esters.[1–4] An area attracting recent attention is the concerted action of multi-zinc sites in promoting the hydrolysis of phosphate esters. In particular, macrocyclic polyamine ligands have been applied extensively in the construction of metal complexes as models for zinc enzymes promoting phosphoryl transfer reactions.[3–16] The high stability of such complexes allows the generation of otherwise unstable deprotonated forms under physiological pH conditions and the resulting metal-bound hydroxide groups then act as nucleophiles in the cleavage process.[3] A further feature of zinc(II) complexes incorporating polyamine macrocycles, which is important if these complexes are to reproduce the function of the enzymes, is their ability to bind reversibly biological substrate mimics, *e.g.* nitrophenyl phosphate (NPP) and other phosphate esters. Stable 1 : 1 adducts were formed for mononuclear, binuclear and trinuclear zinc(II) complexes of, respectively, cyclen, bis(cyclen) and tris(cyclen) macrocycles (cyclen = 1,4,7,10-tetrazaacyclododecane). The substantial increases in affinity constants for NPP that were observed with increasing nuclearity of the complex, *viz.*, $10^{3.3}$, $10^{4.0}$ and $10^{5.8}$ $dm^3\ mol^{-1}$, respectively, have relevance to the function of trizinc phosphatases.[16] In a further interesting example reported by Kimura and co-workers,[12] the binuclear zinc(II) complex formed by an octaazacryptand was shown to react with a phosphomonoester dianion, 4-nitrophenyl phosphate (NPP^{2-}), to produce a phosphoramide derivative. It was anticipated that the complex would be unreactive towards phosphate esters because the zinc(II) centres appear to be co-ordinatively saturated in trigonal bipyramidal (*TBPY*) geometry. Further novel applications of zinc(II) complexes include the recent use of a binuclear zinc complex, incorporating a *p*-xylene bridged bis(cyclen) ligand, as a host molecule capable of recognizing barbiturates in aqueous solution[17] and the demonstration that binuclear zinc(II) complexes derived from bis(cyclam) macrocycles exhibit *in vitro* activity against the HIV virus.[18]

In contrast to binucleating ligands incorporating tetradentate macrocycles, such as cyclen, zinc(II) complexes formed by binucleating ligands derived from the smaller macrocycle 1,4,7-triazacyclononane (tacn) have not been studied widely. We report the zinc(II) co-ordination chemistry of a series of bis(pentadentate) ligands obtained by appending 2-pyridylmethyl groups to bis(tacn) macrocycles (see Scheme 1). Detailed studies of the complexes of Cu^{II}, Ni^{II} and Mn^{II} have been reported previously.[19–22] The crystal structures of two of the

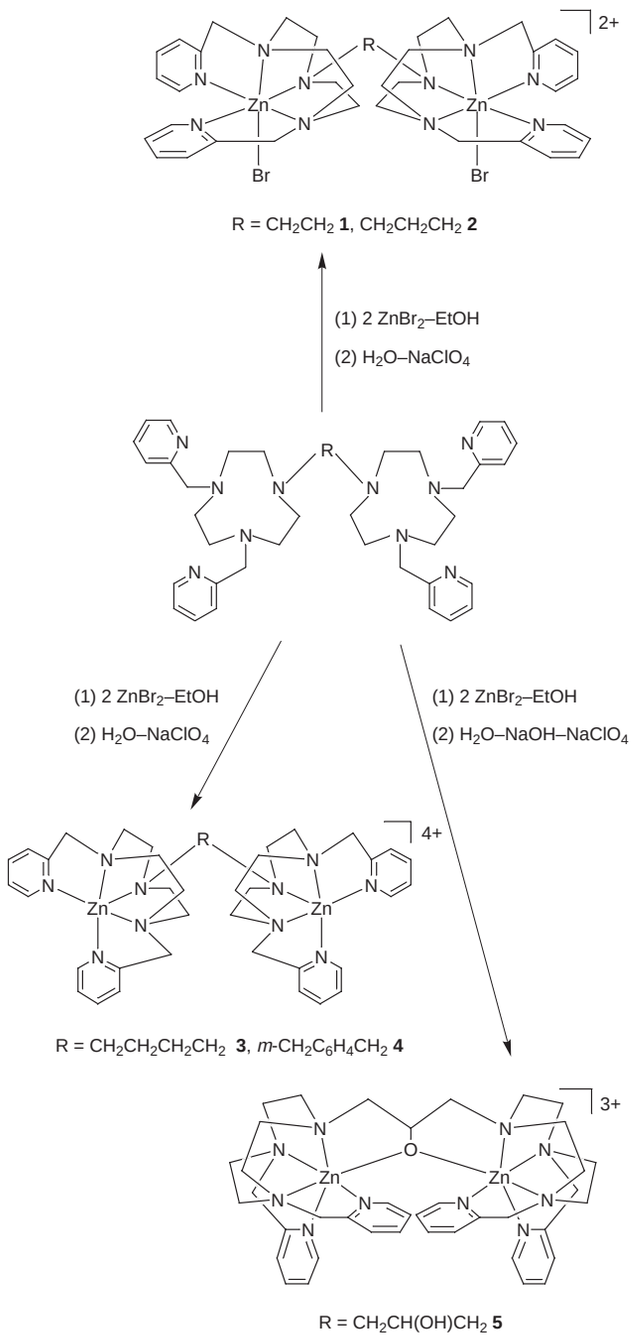

Scheme 1

zinc(II) complexes and solution NMR spectroscopic studies have revealed interesting structural variations in solution and solid state structures.

Experimental

Materials

Reagent or AR grade chemicals were used in this study. Published methods were used to prepare tmpdtne[19] {1,2-bis[4,7-bis(2-pyridylmethyl)-1,4,7-triazacyclonon-1-yl]ethane}, tmpdtnp[19] {1,3-bis[4,7-bis(2-pyridylmethyl)-1,4,7-triazacyclonon-1-yl]propane}, tmpdtnb[19] {1,4-bis[4,7-bis(2-pyridylmethyl)-1,4,7-triazacyclonon-1-yl]butane}, tmpdtn*m*-X[20] {1,3-bis[4,7-bis(2-pyridylmethyl)-1,4,7-triazacyclonon-1-ylmethyl]-benzene} and tmpdtnp-OH[20] {1,3-bis[4,7-bis(2-pyridylmethyl)-1,4,7-triazacyclonon-1-yl]-2-propanol}.

CAUTION: Although no problems were encountered in this work, transition metal perchlorates are potentially explosive and should be handled with due care.

Physical measurements

Proton and ^{13}C NMR spectra were recorded on a Bruker AC200 spectrometer with sodium 3-trimethylsilylpropionate as internal calibrant, IR spectra on a Perkin-Elmer 1600 FTIR spectrometer as KBr pellets. Electron microprobe analyses were made with a JEOL JSM-1 scanning electron microscope through an NEC X-ray detector and pulse processing system connected to a Packard multichannel analyser. Microanalyses were performed by Chemical and Micro-Analytical Services (CMAS) Melbourne, Australia. Conductivity was measured using a Crison 522 Conductimeter with platinum black electrodes. Standard KCl (0.020 M) with a conductivity of 2.77 mS cm^{-1} was used as a calibrant.

Synthesis of complexes

$[Zn_2(tmpdtne)Br_2][ClO_4]_2\cdot H_2O$ 1. To a dark red-brown solution of tmpdtne (1.69 g, 2.61 mmol) in EtOH (20 ml) was added a slight excess of $ZnBr_2$ (1.23 g, 5.48 mmol). The brown precipitate formed was collected and dissolved in a small amount of water (10 ml) with gentle heating to give a dark brown solution. Sodium perchlorate (1.0 g) was added and the resulting solution was allowed to stand. The light brown crystalline product was filtered off and recrystallized from a DMSO–water mixture to give colourless crystals of the monohydrate (yield 1.51 g, 51%). Crystals of the bis(DMSO) solvate suitable for X-ray crystallography deposited from the same solution. {Found: C, 39.9; H, 4.7; N, 12.2. Calc. for $[Zn_2(C_{38}H_{52}N_{10})Br_2][ClO_4]_2\cdot H_2O$: C, 40.1; H, 4.6; N, 12.3%}. Electron microprobe: Cl : Zn : Br ratio 1 : 1 : 1. Selected IR bands (KBr, cm^{-1}): 3570s, 3504s, 2912m, 2870s, 1609s, 1493m, 1444s, 1089vs, 1018s, 770m and 624s. Molar conductivity (DMSO, S cm^2 mol^{-1}): 77 (298) and 121 (363 K). ^{1}H NMR (d_6-DMSO, 363 K): δ 2.54 (s, 8 H, $NC_5H_4CH_2NCH_2CH_2NCH_2C_5H_4N$); 2.55 (m, 4 H, bridge CH_2), 2.80 (m, 8 H, $NC_5H_4CH_2NCH_2CH_2N$ bridge), 2.94 (m, 8 H, $NC_5H_4CH_2NCH_2CH_2N$ bridge), 4.14 (d, 4 H, $CH_2C_5H_4N$), 4.34 (d, 4 H, $CH_2C_5H_4N$); 7.51 (t, 4 H, arylCH), 7.58 (d, 4 H, arylCH) and 8.07 (td, 8 H, arylCH). ^{13}C NMR (d_6-DMSO, 363 K): δ 49.58 (bridge CH_2), 50.01, 51.43, 53.78 (tacn CH_2), 59.72 ($CH_2C_5H_4N$), 123.92, 124.24, 139.97, 146.33 and 154.49 (pyridyl ring C). ESI-mass spectrum (MeOH–water): *m*/*z* 1076.8, $[Zn_2L(ClO_4)_3]^+$; 1058.8, $[Zn_2LBr(ClO_4)_2]^+$; 1038.8, $[Zn_2LBr_2(ClO_4)]^+$; 489.1, $[Zn_2L(ClO_4)_2]^{2+}$; 479.0, $[Zn_2LBr(ClO_4)]^{2+}$; 469.1, $[Zn_2LBr_2]^{2+}$; 293.0, $[Zn_2L(ClO_4)]^{3+}$; and 286.4, $[Zn_2LBr]^{3+}$.

$[Zn_2(tmpdtnp)Br_2][ClO_4]_2\cdot 3H_2O$ 2. To a dark red-brown solution of tmpdtnp (3.5 g, 5.30 mmol) in EtOH (20 ml) was added a slight excess of $ZnBr_2$ (2.51 g, 11.1 mmol) to produce a brown precipitate. This was filtered off, dissolved in a CH_3CN–water mixture with gentle warming and the resulting dark brown solution decolourized twice with activated charcoal to give a yellow filtrate. Sodium perchlorate (2.0 g) was added and the solution was allowed to stand. The white product was filtered off and recrystallized from a CH_3CN–water mixture to give a white powder (yield 2.14 g, 35%). {Found: C, 38.5; H, 4.7; N, 11.4. Calc. for $[Zn_2(C_{39}H_{54}N_{10})Br_2][ClO_4]_2\cdot 3H_2O$: C, 38.8; H, 5.0; N, 11.6%}. Electron microprobe: Cl : Zn : Br ratio 1 : 1 : 1. Selected IR bands (KBr, cm^{-1}): 3455 (br), 2922w, 2859w, 1608s, 1463m, 1443s, 1094vs, 1019m, 765m and 625s. Molar conductivity (DMSO, S cm^2 mol^{-1}): 89 (298) and 149 (363 K). ^{1}H NMR (d_6-DMSO, 363 K): δ 1.36 (br, 2 H, $NCH_2CH_2CH_2N$), 2.71 (m, 8 H, $NC_5H_4CH_2NCH_2CH_2N$ bridge), 2.78 (br, 8 H, $NC_5H_4CH_2NCH_2CH_2NCH_2C_5H_4N$), 2.96 (dd, 8 H, $NC_5H_4CH_2NCH_2CH_2N$ bridge), 2.58 (br, 4 H, $NCH_2CH_2CH_2N$), 4.13 (d, 4 H, $CH_2C_5H_4N$), 4.32 (d, 4 H, $CH_2C_5H_4N$); 7.51 (t, 4 H, arylCH), 7.57 (d, 4 H, arylCH) and 8.09 (td, 8 H, arylCH). ^{13}C NMR (d_6-DMSO, 363 K): δ 21.26 (11), 56.51 (10) (bridge CH_2), 49.83 (1), 50.62 (2), 51.76 (3), (tacn CH_2), 60.30 (4) ($CH_2C_5H_4N$), 123.95 (8), 124.33 (6), 140.06 (7), 146.44 (9) and

154.60 (5) (pyridyl ring C). Fig. 4 shows the spectra and carbon atom assignments. ESI-mass spectrum (MeOH–H_2O): *m/z* 1091.2, $[Zn_2L(ClO_4)_3]^+$; 1071.2, $[Zn_2LBr(ClO_4)_2]^+$; 1051.1, $[Zn_2LBr_2(ClO_4)]^+$; 496.1, $[Zn_2L(ClO_4)_2]^{2+}$; 486.1, $[Zn_2LBr(ClO_4)]^{2+}$; 476.1, $[Zn_2LBr_2]^{2+}$; 297.1, $[Zn_2LBr]^{3+}$; and 291.1, $[Zn_2LBr]^{3+}$.

$[Zn_2(tmpdtnb)][ClO_4]_4\cdot 3DMSO$ 3. The method used to prepare complex **1** was followed but with 2.08 g (3.08 mmol) of tmpdtnb and 1.46 g (6.46 mmol) of $ZnBr_2$. The white solid appeared as colourless crystals when recrystallized from a DMSO–water mixture (yield 1.42 g, 32%). {Found: C, 38.7; H, 5.3; N, 9.1. Calc. for $[Zn_2(C_{40}H_{56}N_{10})][ClO_4]_4\cdot 3DMSO$: C, 38.4; H, 5.1; N, 9.7%}. Electron microprobe: Zn : Cl : S ratio 2 : 4 : 3, no Br present. Selected IR bands (KBr, cm^{-1}): 2919m, 1640m, 1608s, 1465m, 1441s, 1088vs, 1020s, 955m, 769m and 628s. ^1H NMR (d_6-DMSO, 300 K): δ 1.22 (br, 4 H, $NCH_2CH_2CH_2CH_2N$), 2.54 (s, 8 H, $NC_5H_4CH_2NCH_2CH_2NCH_2C_5H_4N$), 2.58 (t, 4 H, $NCH_2CH_2CH_2CH_2N$), 2.77 (m, 8 H, $NC_5H_4CH_2NCH_2CH_2N$ bridge), 3.06 (m, 8 H, $NC_5H_4CH_2NCH_2CH_2N$ bridge), 4.31 (dd, 8 H, $CH_2C_5H_4N$), 7.64 (t, 4 H, arylCH), 7.72 (d, 4 H, arylCH), 7.99 (d, 4 H, arylCH) and 8.21 (td, 4 H, arylCH). ^{13}C NMR (d_6-DMSO, 298 K): δ 22.12, 57.87 (bridge CH_2), 49.98, 50.40, 51.37 (tacn CH_2), 59.51 ($CH_2C_5H_4N$), 124.87, 125.27, 141.14, 147.07 and 155.17 (pyridyl ring C). ESI-mass spectrum (MeOH–water): *m/z* 1105.2, $[Zn_2L(ClO_4)_3]^+$; 503.1, $[Zn_2L(ClO_4)_2]^{2+}$; 301.8, $[Zn_2L(ClO_4)]^{3+}$.

$[Zn_2(tmpdtn$ *m*$-X)][ClO_4]_4$ 4. The method used to prepare complex **1** was followed but with 2.35 g (3.25 mmol) of tmpdtn*m*-X and 1.53 g (6.82 mmol) of $ZnBr_2$. The product was isolated as a white crystalline solid when recrystallized from a DMSO–water mixture (yield 1.22 g, 30%). {Found: C, 42.2; H, 4.5; N, 11.1. Calc. for $[Zn_2(C_{44}H_{56}N_{10})][ClO_4]_4$: C, 42.2; H, 4.5; N, 11.2%}. Electron microprobe: Cl : Zn ratio 2 : 1, no Br present. Selected IR bands (KBr, cm^{-1}): 2921w, 2866w, 1609s, 1485m, 1444s, 1090vs, 1018s, 767m and 626s. ^1H NMR (d_6-DMSO, 300 K): δ 2.73 (m, 16 H, $NC_5H_4CH_2NCH_2CH_2N$ bridge), 2.99 (m, 8 H, $NC_5H_4CH_2NCH_2CH_2N$ bridge), 3.92 (br, 4 H, bridge CH_2), 4.34 (dd, 8 H, $CH_2C_5H_4N$), 7.27 (d, 2 H, bridge arylCH), 7.69 (dd, 2 H, bridge arylCH), 7.54 (d, 4 H, arylCH), 7.60 (t, 4 H, arylCH), 7.73 (d, 4 H, arylCH) and 8.21 (td, 4 H, arylCH). ^{13}C NMR (d_6-DMSO, 300 K): δ 48.09, 50.68, 51.20, (tacn CH_2), 58.25, ($NC_5H_4CH_2$) 60.10 (xylylene CH_2), 124.73, 125.26, 141.37, 147.15, 155.02 (pyridyl ring C), 127.82, 131.25, 133.27 and 134.36 (benzene ring C). ESI-mass spectrum (MeOH–water): *m/z* 1153.2, $[Zn_2L(ClO_4)_3]^+$; and 527.1, $[Zn_2L(ClO_4)_2]^{2+}$.

$[Zn_2(tmpdtnp\text{-}O)][ClO_4]_3\cdot 0.5H_2O$ 5. The method used to prepare complex **1** was followed with 2.50 g (3.69 mmol) of tmpdtnp-OH and 1.75 g (7.75 mmol) of $ZnBr_2$. On the addition of 2 M NaOH to the yellow filtrate a white microcrystalline solid formed. This was recrystallized from a CH_3CN–water mixture to give rectangular shaped colourless crystals suitable for X-ray diffraction (Yield 1.67 g, 41%). {Found: C, 42.4; H, 5.1; N, 12.8. Calc. for $[Zn_2(C_{39}H_{53}N_{10}O)][ClO_4]_3\cdot 0.5H_2O$: C, 42.0; H, 4.9; N, 12.6%}. Electron microprobe: Cl : Zn ratio 3 : 2, no Br present. Selected IR bands (KBr, cm^{-1}): 3577s, 3453 (br), 2926s, 2861s, 1610s, 1470s, 1446s, 1078vs, 1021s, 1003s, 764s and 624s. ^1H NMR (d_6-DMSO, 300 K): δ 1.25 [m, 2 H, CH(H_a)CHOHCH(H_a)], 1.77 [m, 2 H, CH(H_b)CHOHCH(H_b)], 2.34 (m, 1 H, C*H*OH), 2.70 (m, 8 H, $NC_5H_4CH_2NCH_2CH_2N$ bridge), 3.00 (m, 8 H, $NC_5H_4CH_2NCH_2CH_2N$ bridge), 3.20 (s, 8 H, $NC_5H_4CH_2NCH_2CH_2NCH_2C_5H_4N$), 3.58 (dd, 4 H, $CH_2C_5H_4N$), 4.18 (dd, 4 H, $CH_2C_5H_4N$), 7.09 (t, 2 H, arylCH), 7.19 (d, 2 H, arylCH), 7.29 (d, 2 H, arylCH), 7.59 (t, 2 H, arylCH), 7.68 (d, 2 H, arylCH), 7.93 (td, 2 H, arylCH), 8.26 (td, 2 H, arylCH) and 8.91 (d, 2 H, arylCH). ^{13}C NMR (d_6-DMSO, 300 K): δ 49.91(1), 50.83 (1), 51.55 (3), 54.49 (4), 55.19 (5), 57.73 (6) (tacn ring CH_2), 62.22 (7), 62.73 (13) ($CH_2C_5H_4N$), 64.83 (19), 66.91 (20) (bridge CH_2), 124.71 (9), 124.76 (15), 124.82 (11), 125.98 (17), 141.27 (10), 141.51 (16), 146.26 (12), 149.13 (18), 154.85 (8) and 156.20 (14) (pyridyl ring C). The spectra and signal assignments are shown in Fig. 5. ESI-mass spectrum (MeOH–water): *m/z* 1007.0, $[Zn_2(tmpdtnp\text{-}O)(ClO_4)_2]^+$; 453.2, $[Zn_2(tmpdtnp\text{-}O)(ClO_4)]^{2+}$; and 269.8, $[Zn_2(tmpdtnp\text{-}O)]^{3+}$.

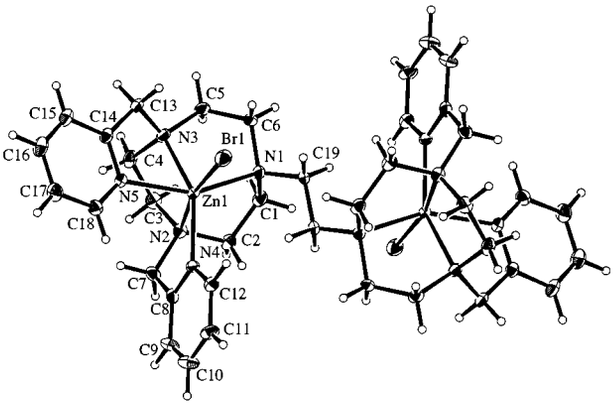

Fig. 1 Molecular structure of the dinuclear cation in $[Zn_2(tmpdtne)Br_2][ClO_4]_2\cdot 2DMSO$ **1** and atom labelling scheme (ellipsoids are drawn at 20% probability).

Crystallography

Intensity data for a colourless prismatic crystal of complex **1** ($0.36 \times 0.28 \times 0.14$ mm) and a multifaceted pale yellow crystal ($0.23 \times 0.23 \times 0.36$ mm) of **5** were collected on Rigaku diffractometers (AFC6S for **1** and AFC6R for **5**) employing Mo-Kα radiation and the ω–2θ scan technique. The data sets were corrected for Lorentz-polarization effects[23] as well as for absorption employing an empirical procedure.[24] In the case of **5** the data set was scaled assuming a linear decay owing to some decomposition of the crystal noted during the data collection (*ca.* 10%). Crystal data and refinement details are given in Table 1.

The structures were solved by direct methods[25] and refined by a full-matrix least-squares procedure based on *F*.[23] Non-hydrogen atoms were generally refined with anisotropic displacement parameters and hydrogen atoms included in the model at their calculated positions (C–H 0.97 Å). For both complexes **1** and **5**, disorder was noted for one of the perchlorate anions such that two sites were identified for three of the oxygen atoms, *i.e.* O(3)–O(5). Refinement (isotropic) indicated an occupancy distribution of 50/50, and 59/41% for **1** and **5**, respectively. Additionally, disorder was noted in the oxygen atoms O(10)–O(13) in the refinement of **5**; these atoms were refined isotropically. Attempts to resolve multiple sites were unsuccessful. The refinement was continued until convergence employing weights, $1/\sigma^2(F)$. The absolute structure of **5** was determined by comparing the refinements of the alternate hands. The results of the refinement that yielded the lower value of R' are presented here. The crystallographic numbering schemes employed are shown in Figs. 1 (**1**) and 2 (**5**).[26]

CCDC reference number 186/1370.

See http://www.rsc.org/suppdata/dt/1999/1475/ for crystallographic files in .cif format.

Results and discussion

Synthesis and solid state characterization

The synthesis of the binuclear zinc(II) complexes of tmpdtne, tmpdtnp, tmpdtnb and tmpdt*m*-X is shown in Scheme 1. Generally, this involved dissolution of the ligands in EtOH and addition of an excess of $ZnBr_2$. The resulting brown precipitates were dissolved in the minimum volume of water and the

complexes precipitated as light brown solids on addition of excess of $NaClO_4$. Recrystallization from either CH_3CN–water or DMSO–water mixtures gave the pure products and, in the case of **1**, crystals suitable for crystallography. As for **1–4**, the synthesis of **5** initially involved reaction of the ligand with excess of $ZnBr_2$. However, following dissolution in the minimum volume of water and addition of $NaClO_4$, sodium hydroxide was added, resulting in the immediate formation of a microcrystalline precipitate. Recrystallization from a CH_3CN–water mixture gave colourless crystals suitable for crystallography. The IR spectra of **1–5** confirmed the presence of the ligands (in particular, pyridyl skeletal vibrations in the 1400–1600 cm^{-1} region were diagnostic of the ligands), perchlorate counter ions, and in some case solvents of crystallization.

Despite the use of zinc bromide in each synthesis, interesting compositional differences are apparent for the five compounds, which cannot be ascribed to changes in the solvents chosen for recrystallization. For both **1** and **2** bromide is present in the products with microprobe analyses confirming Zn : Cl : Br ratios of *ca.* 1 : 1 : 1. In contrast, bromide is absent in the zinc(II) complexes of tmpdtnb, tmpdtn*m*-X and tmpdtnp-OH (**3–5**). For example, microprobe analysis of **3** revealed the presence of Zn, Cl and S (from DMSO) in a ratio of *ca.* 2 : 4 : 3 and no bromide. This finding was in accordance with the elemental analysis, which indicated the presence of three DMSO molecules per complex cation. Bromide was also absent in the tmpdtn*m*-X complex, **4**, but Zn and Cl were detected in a ratio of *ca.* 1 : 2. Elemental analyses support the formation of a five-co-ordinate complex, although solid state zinc(II)–perchlorate counter-ion interactions cannot be excluded. NMR spectroscopy (see later) and the ESI mass spectra of **3** and **4** support this interpretation. The mass spectra showed isotope splitting patterns corresponding to $[Zn_2L(ClO_4)_3]^+$ (1105.2 **3** and 1153.2 **4**); $[Zn_2L(ClO_4)_2]^{2+}$ (503.1 **3** and 527.1 **4**); and $[Zn_2L(ClO_4)]^{3+}$ (301.8 **3**).

The composition of complex **5** is supported by microprobe analysis, which confirmed the absence of bromide and a Zn:Cl ratio of *ca.* 2 : 3. The ESI mass spectrum shows isotope splitting patterns assignable to the cation and cation–ClO_4^- ion pairs, *viz.* $[Zn_2L(ClO_4)_2]^+$ (1007.0), $[Zn_2L(ClO_4)]^{2+}$ (453.2) and $[Zn_2L]^{3+}$ (269.8). The existence of the 3+ cation indicated that the two zinc centres may be bridged by an alkoxide generated from the ligand backbone.

Molecular structures of complexes 1 and 5

The centrosymmetric binuclear cation in complex **1** consists of two six-co-ordinate zinc(II) centres, each complexed by five of the nitrogen donor atoms of the tmpdtne ligand, with a bromide ion in the sixth co-ordination position (Fig. 1). The N(2) and Br atoms in **1** may be viewed as occupying the axial sites of the distorted octahedral geometry while the N(1), N(3), N(4) and N(5) atoms occupy equatorial positions. The stereochemistry about the zinc(II) centres in **1** is similar to that observed in the manganese(II) analogue, $[Mn_2(tmpdtne)Cl_2][ClO_4]_2\cdot 2DMF$,[22] which shows the halide groups to be co-ordinated *cis* rather than *trans* to the bridgehead nitrogens, N(1), *viz.* isomer B rather than A shown in Fig. 3. This asymmetry will be considered further in the analysis of the NMR spectra of **1** and **2** (see below).

The two five-membered chelate rings incorporating the pyridine rings are puckered, as shown by the values of the Zn/N(2)/C(7)/C(8) and Zn/N(3)/C(13)/C(14) torsion angles of −40.8(7)° and −47.0(7)°, respectively. Similar torsion angles of −38.1° and −47.0° were observed in the manganese(II) analogue. The two pyridine rings in complex **1** are fixed at right angles to one another and adopt a Δ configuration. The two halves of the ligand are oriented away from one another in an *anti* configuration. This gives rise to an intramolecular Zn ··· Zn distance of 6.545(9) Å, which is 0.27 Å shorter than in the manganese(II) analogue.[22] This difference in M ··· M distances is not due to changes in the orientation of the two halves of each complex but is most likely to be due to the larger ionic radius of Mn^{II} (0.97 Å), *cf.* Zn^{II} (0.88 Å),[27] a difference which gives rise to longer M–N distances in the manganese complex (average 2.31 Å), *cf.* **1** (2.21 Å).

The bonds connecting the zinc(II) centres to the pyridine and tacn nitrogens span the range 2.14–2.25 Å (Table 2) but are typical of zinc(II)–amine complexes.[11,28,29] Distortion from octahedral geometry is highlighted by the N(1)–Zn–N(5), N(3)–Zn–N(4) and N(2)–Zn–Br angles of 153.7(2), 148.1(2) and 169.2(1)° respectively, which are considerably less than 180°. Slightly greater deviations were evident in the manganese(II) analogue.[22] These distortions from octahedral geometry are largely due to the constraints imposed by each half of the ligand in forming five fused 5-membered chelate rings and steric effects contributed by the bulk and orientation of the pyridine rings (see Fig. 1).

The structure of complex **5** comprises one dinuclear unit, three perchlorate anions and half a molecule of solvent water. The closest non-hydrogen contact in the lattice [*i.e.* not involving the disordered components of the $Cl(1)O_4$ anion] of 2.70(3) Å occurs between O(12) and $O(14^i)$, *i.e.* solvent water molecule, atoms; symmetry operation i $-0.5 + x$, $0.5 - y$, $1 - z$. The O(9) atom also forms a contact of 2.94(3) Å with the $O(14^{ii})$ atom; ii $1 - x$, $-0.5 + y$, $0.5 - z$. The closest non-hydrogen contact between the ions occurs between the

Table 1 Crystallographic data for $[Zn_2(tmpdtne)Br_2][ClO_4]_2\cdot 2DMSO$ **1** and $[Zn_2(tmpdtnp\text{-}O)][ClO_4]_3\cdot 0.5H_2O$ **5**

	1	**5**
Formula	$C_{42}H_{64}Br_2Cl_2N_{10}O_{10}S_2Zn_2$	$C_{39}H_{54}Cl_3N_{10}O_{13.5}Zn_2$
M	1294.62	1116.0
Crystal system	Triclinic	Orthorhombic
Space group	$P\bar{1}$(no. 2)	$P2_12_12_1$ (no. 19)
a/Å	8.103(1)	18.863(9)
b/Å	13.576(2)	19.011(5)
c/Å	13.987(2)	12.663(6)
α/°	111.59(1)	
β/°	105.18(1)	
γ/°	95.82(1)	
V/Å^3	1346.9(4)	4540(2)
Z	1	4
T/K	296	220
λ/Å	0.7107 (Mo-Kα)	0.7107 (Mo-Kα)
D_c/g cm^{-3}	1.596	1.632
$F(000)$	662.0	2308
μ(Mo-Kα)/cm^{-1}	26.17	26.23
No. data measured	5143	5840
No. unique data	4774	5840
No. observed data [$I \geqslant 3\sigma(I)$]	3415	3195
R	0.055	0.072
R'	0.070	0.067
Maximum $\Delta\rho$/e Å^{-3}	1.42	0.95

Table 2 Selected bond distances (Å) and angles (°) for $[Zn_2(tmpdtne)Br_2][ClO_4]_2$ **1**

Zn–Br	2.501(1)	Zn–N(3)	2.211(6)
Zn–N(1)	2.244(5)	Zn–N(4)	2.139(5)
Zn–N(2)	2.247(6)	Zn–N(5)	2.216(6)
Br–Zn–N(1)	93.3(2)	Br–Zn–N(2)	169.2(1)
Br–Zn–N(3)	108.9(2)	Br–Zn–N(4)	99.1(2)
Br–Zn–N(5)	86.5(2)	N(1)–Zn–N(2)	79.6(2)
N(1)–Zn–N(3)	81.0(2)	N(1)–Zn–N(4)	112.9(2)
N(1)–Zn–N(5)	153.7(2)	N(2)–Zn–N(3)	78.3(2)
N(2)–Zn–N(4)	76.5(2)	N(2)–Zn–N(5)	103.5(2)
N(3)–Zn–N(4)	148.1(2)	N(3)–Zn–N(5)	74.3(2)
N(4)–Zn–N(5)	93.0(2)		

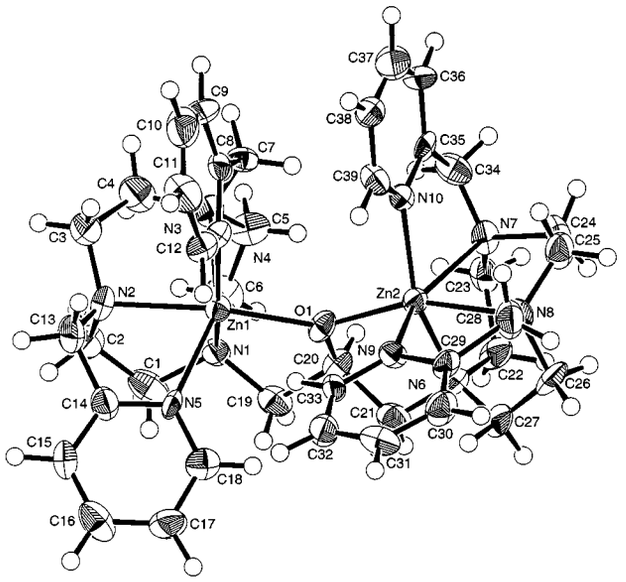

Fig. 2 Molecular structure of the dinuclear cation in $[Zn_2(tmpdtnp\text{-}O)][ClO_4]_3\cdot 0.5H_2O$ **5** and atom labelling scheme (ellipsoids are drawn at 50% probability).

Table 3 Selected bond distances (Å) and angles (°) for $[Zn_2(tmpdtnp\text{-}O)][ClO_4]_3\cdot 0.5H_2O$ **5**

Zn(1)–O(1)	2.062(9)	Zn(2)–O(1)	2.10(1)
Zn(1)–N(1)	2.11(1)	Zn(2)–N(6)	2.17(1)
Zn(1)–N(2)	2.27(1)	Zn(2)–N(7)	2.31(1)
Zn(1)–N(3)	2.24(1)	Zn(2)–N(8)	2.24(1)
Zn(1)–N(4)	2.09(1)	Zn(2)–N(9)	2.17(1)
Zn(1)–N(5)	2.28(1)	Zn(2)–N(10)	2.12(1)
O(1)–Zn(1)–N(1)	82.3(4)	O(1)–Zn(2)–N(6)	82.4(4)
O(1)–Zn(1)–N(2)	162.4(5)	O(1)–Zn(2)–N(7)	110.5(4)
O(1)–Zn(1)–N(3)	99.3(4)	O(1)–Zn(2)–N(8)	159.2(4)
O(1)–Zn(1)–N(4)	100.9(4)	O(1)–Zn(2)–N(9)	96.3(4)
O(1)–Zn(1)–N(5)	106.9(4)	O(1)–Zn(2)–N(10)	105.2(4)
N(1)–Zn(1)–N(2)	80.1(5)	N(6)–Zn(2)–N(7)	78.6(4)
N(1)–Zn(1)–N(3)	81.1(4)	N(6)–Zn(2)–N(8)	81.1(5)
N(1)–Zn(1)–N(4)	160.3(4)	N(6)–Zn(2)–N(9)	104.1(4)
N(1)–Zn(1)–N(5)	93.6(5)	N(6)–Zn(2)–N(10)	154.4(4)
N(2)–Zn(1)–N(3)	78.4(4)	N(7)–Zn(2)–N(8)	78.4(4)
N(2)–Zn(1)–N(4)	95.8(5)	N(7)–Zn(2)–N(9)	153.1(4)
N(2)–Zn(1)–N(5)	74.0(4)	N(7)–Zn(2)–N(10)	75.8(5)
N(3)–Zn(1)–N(4)	79.2(5)	N(8)–Zn(2)–N(9)	75.7(4)
N(3)–Zn(1)–N(5)	152.4(4)	N(8)–Zn(2)–N(10)	95.1(4)
N(4)–Zn(1)–N(5)	103.8(5)	N(9)–Zn(2)–N(10)	99.4(4)

O(2) and C(9^{iii}) atoms of 3.09(3) Å; notably O(2) is the only ordered oxygen atom of the Cl(1)O_4 anion; iii $0.5 - x$, $1 - y$, $0.5 + z$.

The structure of the $[Zn_2(tmpdtnp\text{-}O)]^{3+}$ cation in complex **5** shows that deprotonation of the $CH_2CH(OH)CH_2$ ligand backbone has occurred and that the two zinc centres are bridged by the resulting alkoxo group (Fig. 2). This behaviour contrasts with that of the copper(II) analogue where deprotonation and co-ordination of the $CH_2CH(OH)CH_2$ backbone is not supported by the analytical and magnetic data.[20] The Zn···Zn separation in **5** [3.903(2) Å] closely matches the value of 3.94 Å established for the dizinc active site of alkaline phosphatase.[5,30] In contrast, a related alkoxo-bridged zinc(II) model complex incorporating an octaazacryptand exhibits a much shorter Zn···Zn distance of 3.42 Å.[12] Asymmetry in **5** is introduced by the perpendicular arrangement of the two 2-pyridylmethyl pendant arms on each zinc centre and the *cis*-disposition of the bridging oxygen relative to the bridgehead nitrogens, N(1) and N(6).

The co-ordination sphere of each zinc(II) centre is occupied by five nitrogen donors and the oxygen from the bridging alkoxide from the ligand, creating a distorted octahedral geometry.

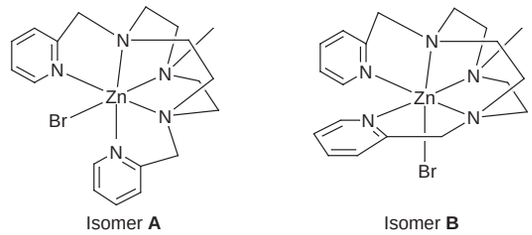

Fig. 3 Isomers arising from positioning of bromide ligand *trans* (**A**) and *cis* (**B**) to the bridgehead nitrogen.

The Zn(1)–O(1) and Zn(2)–O(1) bond lengths of 2.062(9) and 2.10(1) Å (Table 3), respectively, are shorter than the Zn–N bonds (average 2.2 Å). Even shorter Zn–O bonds of 1.93 Å were observed in the zinc(II) complex of a propanol-bridged octaazacryptand.[12] The steric limitations of the ligand cause the apical angles in **5** to be bent at 162.4(5)° for O(1)–Zn(1)–N(2) and 159.2(4)° for O(1)–Zn(2)–N(8). The chelate rings involving the 2-pyridylmethyl arms are puckered as shown by the torsion angles of −52(1) and −44(1)° for Zn(1)–N(2)–C(13)–C(14) and Zn(1)–N(3)–C(7)–C(8), and 42(1) and 38(1)° for Zn(2)–N(8)–C(28)–C(29) and Zn(2)–N(7)–C(34)–C(35). Despite the constraints introduced by the rigidity of the alkoxo bridge these torsion angles are similar to those observed for **1** (see above).

Solution NMR spectroscopic examination of complexes 1–5

A detailed NMR study of complexes **1–5** has identified some interesting spectral variations, which can be ascribed to changes in structure in solution. At room temperature the ^{1}H NMR spectra of **1** and **2** run in d_6-DMSO exhibit broad signals (spectra for **2** are shown in Fig. 4) suggesting that the CH_2 and CH protons exchange between different environments on the NMR timescale. The sharper signal due to d_5-DMSO (a contaminant in the deuteriated solvent) indicates either that it is not co-ordinated or that co-ordinated d_5-DMSO exchanges rapidly with the bulk solvent.

In an attempt to resolve the overlapping signals within the ^{1}H NMR spectra of complexes **1** and **2**, spectra were recorded at 363 K (the freezing point of DMSO and insufficient solubility in other solvents prevented lower temperature NMR studies). The resulting spectra exhibit sharper, readily assignable signals (see Fig. 4). The tacn ring protons of each complex (signals **1–3**) appear as multiplets in the δ 2.5–3.3 region while the bridging methylene protons appear at δ 2.80 (**1**), and 2.58 and 1.36 (**2**). For both complexes, the mutually coupled CH_2 protons connecting the pyridine rings to the tacn macrocycle (signals 4) form an AB system and thus appear as a doublet of doublets centred at δ 4.14 (**1**) and 4.32 (**2**). The aromatic protons of the pyridine rings appear between δ 7.5 and 8.1. Complex **2** exhibits a triplet at δ 7.51 [H(8) protons], a doublet at δ 7.57, [H(6) protons] and two overlapping signals at δ 8.09 [H(7), triplet; H(9), doublet]. Twice the number of signals are found in the aromatic region of the cobalt(III) analogues.[31] Thus, while isomer B (Fig. 3) is stabilized in the solid state for both **1**, **2** and the cobalt(III) analogues, in solution this stereochemistry is preserved only for the cobalt(III) complex. In DMSO at 363 K the zinc(II) complexes adopt a structure which essentially preserves the symmetry of the ligand.

The *J*-modulated ^{13}C NMR spectra of complexes **1** and **2**, also run at 363 K, showed clear and sharp signals allowing each unique carbon atom to be assigned (see Fig. 4 for spectrum of **2**) in each complex. Half the signals are observed for **1**, *cf*. the cobalt(III) analogue, further confirming that a more symmetric geometry is adopted in solution at elevated temperatures.

Two important questions about the NMR spectra of complexes **1** and **2** need addressing: (i) why are the number of resonances observed only half of those seen for the cobalt(III)

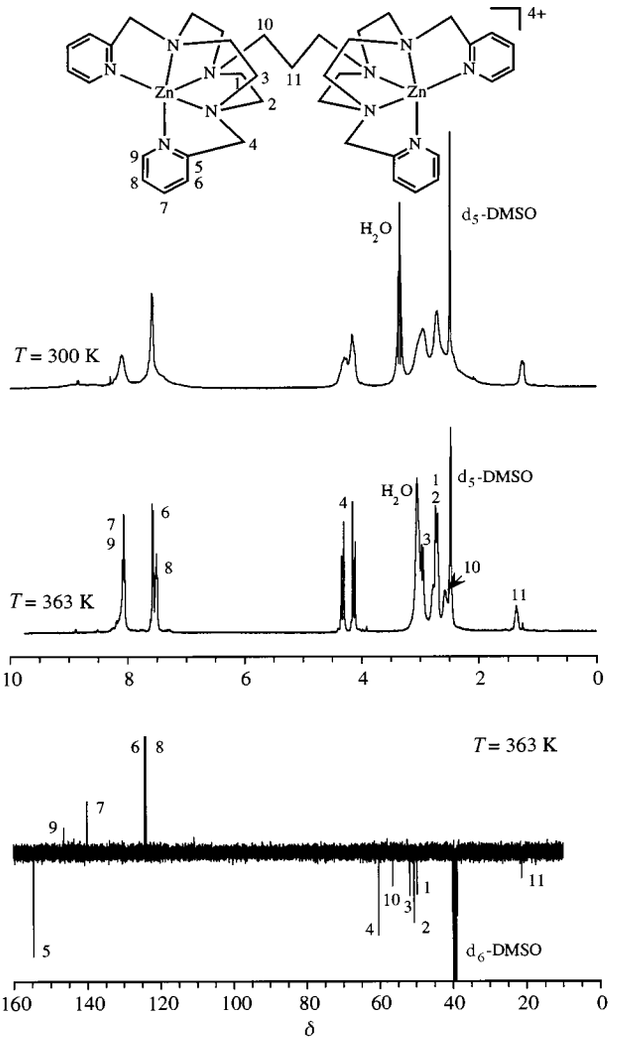

Fig. 4 Proton and ^{13}C NMR spectra of $[Zn_2(tmpdtnp)Br_2][ClO_4]_2$ **2** run in d_6-DMSO at either 300 or 363 K.

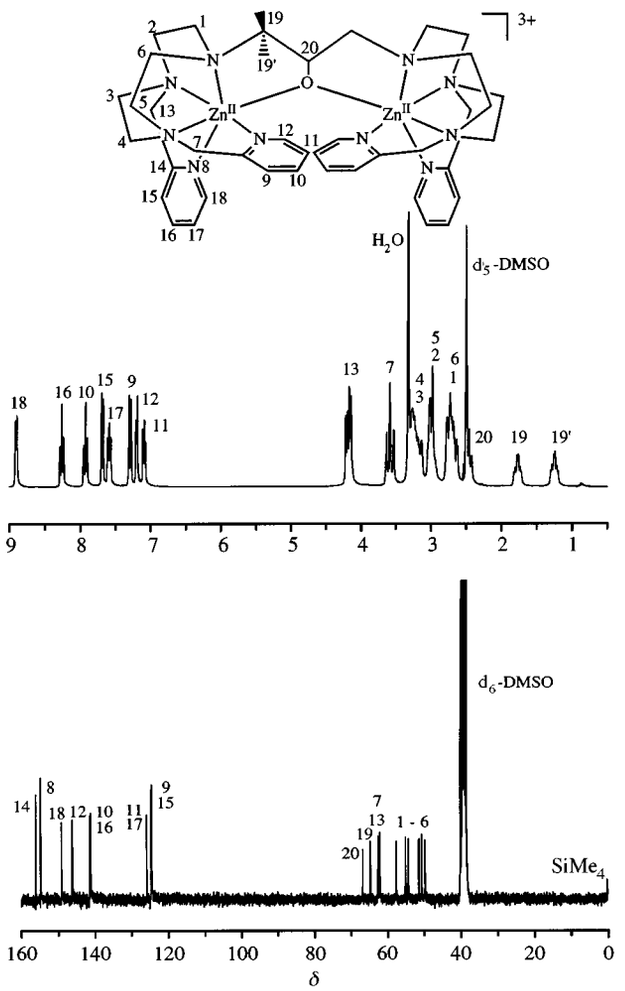

Fig. 5 Proton and ^{13}C NMR spectra of $[Zn_2(tmpdtnp\text{-}O)][ClO_4]_3$ **5** run in d_6-DMSO at either 300 or 363 K.

analogues; (ii) why do the signals become sharper when the temperature is increased?

The crystal structure of complex **1** shows that the bromide ions are co-ordinated *cis* to the bridgehead nitrogen, N(1), such that the arrangement of the ligand around each zinc(II) centre is asymmetrical with the two chelate rings involving the pyridine rings being inequivalent. If the zinc(II) complex were to retain this geometry in solution, the ^1H and ^{13}C NMR spectra should be sharp and exhibit twice as many resonances as found for $[Co_2(tmpdtne)Cl_2][ClO_4]_4$.[31] For both complexes, it is possible that in solution at 363 K DMSO binds at a position *trans* to the bridgehead nitrogen (Scheme 2a). This would require replacement of the bromide ligands, which prefer to bind *cis* to the bridgehead nitrogen. This may also have been expected to give rise to broad signals due to DMSO (partly deuteriated). Our preferred interpretation is that the bromide anions are released from the zinc(II) centres and that this results in a square-pyramidal zinc(II) geometry with the bridgehead nitrogen in the apical position (Scheme 2b). The structures of the copper(II) complexes of several of these ligands clearly highlight their preference for forming square-planar five-co-ordinate complexes. For the cobalt(III) complexes, slow exchange kinetics and a lower propensity to reduce coordination number make this unlikely.

The room temperature ^1H NMR signals are broadened because of exchange between different conformations of the complex. An equilibrium (1) is established between various

$$[Zn_2LBr_2]^{2+} \rightleftharpoons [Zn_2LBr]^{3+} \rightleftharpoons [Zn_2L]^{4+} \qquad (1)$$

forms of each complex and these interconvert on the NMR timescale. However, when the solution is heated the equilibrium is shifted to the right and the number of ^1H NMR signals indicates that the pyridine rings are arranged symmetrically around the zinc(II) centres, as was found in the crystal structures of the copper(II) complexes.[19,20] The ESI mass spectra confirm that species corresponding to the loss of one or both bromides can be generated *viz.* $[Zn_2LBr(ClO_4)_2]^+$ and $[Zn_2L(ClO_4)_3]^+$. An increase in conductivity from ≈ 80 S cm^2 mol^{-1} at 300 K to ≈ 130 S cm^2 mol^{-1} at 363 K supports this conclusion.

In contrast to complexes **1** and **2**, the ^1H NMR spectra of **3** and **4** were resolved at 300 K. In particular, the aromatic region for **3** corresponds well to that of **1** and **2** at 363 K while that of **4** also exhibits signals due to the *m*-xylyl ring. For these complexes, the more symmetric geometry is adopted even at room temperature. Within the series of complexes **1–5**, the spacers joining the two halves of the ligand are longest in **3** and **4** and it would be anticipated that these complexes would have longer Zn···Zn separations. It may then be postulated that, due to reduced electrostatic effects, the equilibrium (1) favours the higher charged species for **3** and **4** (*i.e.* moves to the right). Thus, **1–4** follow a consistent pattern in that the complexes with anticipated shorter Zn···Zn separations (**1**, **2**) exhibit fluxional behaviour at room temperature which is no longer evident for those with longer Zn···Zn separations (**3**, **4**).

The room temperature ^1H and ^{13}C NMR spectra of complex **5** (Fig. 5) are different to those of **1–4** in that they exhibit twice the number of signals. The CH_2 protons of the propoxide bridge are in different environments and couple to each other

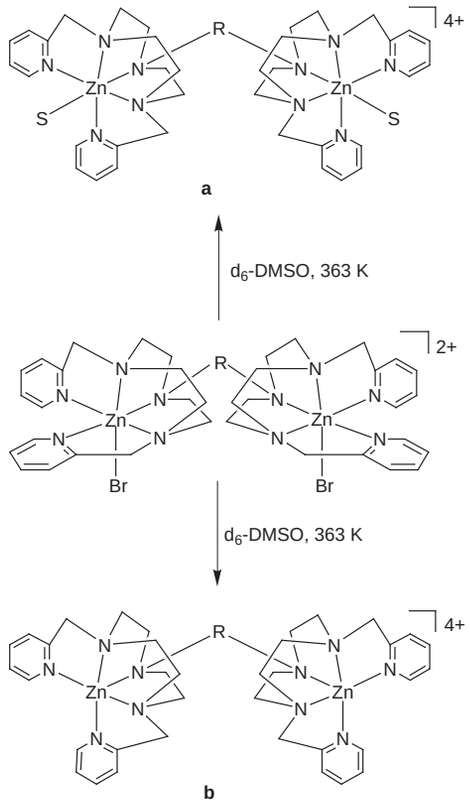

Scheme 2 Possible structural rearrangement of zinc(II) complexes in DMSO solution.

and the central CH proton in the bridge. As was found for the tmpdtnp-OH ligand, this gives rise to multiplets at δ 1.25 and 1.77. A multiplet at δ 2.34 corresponds to the central CH proton of the propoxide bridge. Since the bridging alkoxo group is located *cis* to the bridgehead nitrogen (essentially isomer **A** in Fig. 3 is generated), the carbons within each half of the ligand are inequivalent and give rise to separate ^{13}C NMR signals. A further consequence of this is that each set of CH_2 on the tacn rings and CH protons of the pyridyl rings gives rise to different signals and, thus, twice the number of signals are observed when compared to those of **3** and **4**.

Conclusion

The series of zinc(II) complexes presented here have been found to display interesting variations in their solid state and solution stereochemistry. In one example, the asymmetric arrangement of donor atoms within the octahedral co-ordination sphere of Zn^{II} observed in the solid state is replaced by a more symmetric solution geometry (possibly square pyramidal through loss of the halide ligand) at elevated temperatures. At lower temperatures broad ^{1}H NMR signals indicated rearrangement between different structures on the NMR timescale. As the bridge linking the two pentadentate compartments of the ligands is lengthened, the more symmetric stereochemistry is adopted even at room temperature. This particular property of these complexes could well be exploited in hydrolytic studies related to the function of various zinc bio-sites.

A bridged binuclear zinc(II) complex has been generated for the tmpdtnp-OH ligand in which an endogenous alkoxide group, formed by deprotonation of the 2-propanol backbone, links the two zinc(II) centres. This is in contrast to the analogous copper(II) complex for which there is no evidence of deprotonation and co-ordination of the $CH_2CH(OH)CH_2$ group.[20] The intramolecular Zn···Zn separation of 3.904(2) Å is in agreement with the M···M separation observed for the active site of alkaline phosphatase.[5,30]

Acknowledgements

We thank the Australian Research Council for support of the work at Monash University (to L. S.) and the crystallographic facility at the University of Adelaide (E. R. T. T.). S. J. B. was the recipient of a Monash Graduate Scholarship. We thank Dr Jo Weigold for assistance with the NMR experiments.

References

1 S. J. Lippard and J. M. Berg, *Principles of Bioinorganic Chemistry*, University Science Books, Mill Valley, 1994.
2 W. Kaim and B. Schwederski, *Bioinorganic Chemistry*, Wiley, Chichester, 1994.
3 E. Kimura, *Prog. Inorg. Chem.*, 1994, **41**, 443; E. Kimura, T. Koike and M. Shionoya, *Struct. Bonding* (*Berlin*), 1997, **90**, 1.
4 N. Sträter, W. N. Lipscomb, T. Klabunde and B. Krebs, *Angew. Chem., Int. Ed. Engl.*, 1996, **35**, 2024; D. Gani and J. Wilkie, *Struct. Bonding* (*Berlin*), 1997, **90**, 133.
5 T. Tanase, J. W. Yun and S. J. Lippard, *Inorg. Chem.*, 1996, **35**, 3585; 4220.
6 E. Kimura, T. Shiota, T. Koike and M. Shiro, *J. Am. Chem. Soc.*, 1990, **112**, 5805.
7 T. Koike and E. Kimura, *J. Am. Chem. Soc.*, 1991, **113**, 8935.
8 T. Koike, E. Kimura, I. Nakamura, Y. Hashimoto and M. Shiro, *J. Am. Chem. Soc.*, 1992, **114**, 7338.
9 M. J. Young and J. Chin, *J. Am. Chem. Soc.*, 1995, **117**, 10577.
10 W. H. Chapman, Jr. and R. Breslow, *J. Am. Chem. Soc.*, 1995, **117**, 5642.
11 T. Koike, S. Kajitani, I. Nakamura, E. Kimura and M. Shiro, *J. Am. Chem. Soc.*, 1995, **117**, 1210.
12 T. Koike, M. Inoue, E. Kimura and M. Shiro, *J. Am. Chem. Soc.*, 1996, **118**, 3091.
13 K. A. Deal, A. C. Hengge and J. K. Burstyn, *J. Am. Chem. Soc.*, 1996, **118**, 1713; K. A. Deal and J. N. Burstyn, *Inorg. Chem.*, 1996, **35**, 2792.
14 C. Bazzicalupi, A. Bencini, A. Bianchi, V. Fusi, C. Giorgi, P. Paoletti, B. Valtancoli and D. Zanchi, *Inorg. Chem.*, 1997, **36**, 2784.
15 P. Molenveld, S. Kapsabelis, J. F. J. Engbersen and D. N. Rheinhoudt, *J. Am. Chem. Soc.*, 1997, **119**, 2948.
16 E. Kimura, S. Aoki, T. Koike and M. Shiro, *J. Am. Chem. Soc.*, 1997, **119**, 3068.
17 T. Koike, M. Takashige, E. Kimura, H. Fujioka and M. Shiro, *Chem. Eur. J.*, 1996, **2**, 617; H. Fujioka, T. Koike, N. Yamada and E. Kimura, *Heterocycles*, 1996, **42**, 775.
18 Y. Inouye, T. Kanamori, M. Sugiyama, T. Yoshida, T. Koike, M. Shionoya, K. Enomoto, K. Suehiro and E. Kimura, *Antiviral Chem. Chemotherapy*, 1995, **6**, 337.
19 S. J. Brudenell, L. Spiccia and E. R. T. Tiekink, *Inorg. Chem.*, 1996, **35**, 1974.
20 S. J. Brudenell, L. Spiccia, A. M. Bond, P. Comba and D. C. R. Hockless, *Inorg. Chem.*, 1998, **37**, 3705.
21 S. J. Brudenell, L. Spiccia, A. M. Bond, P. C. Mahon and D. C. R. Hockless, *J. Chem. Soc., Dalton Trans.*, 1998, 3705.
22 S. J. Brudenell, L. Spiccia, A. M. Bond, P. C. Mahon, G. D. Fallon, D. C. R. Hockless and E. R. T. Tiekink, *Inorg. Chem.*, submitted.
23 TEXSAN, Structure Analysis Package, Molecular Structure Corporation, Houston, TX, 1992.
24 N. Walker and D. Stuart, *Acta Crystallogr., Sect. A*, 1983, **39**, 158.
25 P. T. Beurkens, G. Admiraal, G. Beurskens, W. P. Bosman, S. García-Granda, J. M. M. Smits and C. Smykalla, The DIRDIF program system, Technical Report of the Crystallography Laboratory, University of Nijmegen; DIRDIF 94 (1994) was used for **1** and DIRDIF 92 (1992) for **5.**
26 C. K. Johnson, ORTEP II, Report ORNL-5136, Oak Ridge National Laboratory, Oak Ridge, TN, 1976.
27 F. A. Cotton and G. Wilkinson, *Advanced Inorganic Chemistry*, 5th edn. Wiley, New York, 1988, p. 745.
28 D. Ellis, L. J. Farrugia, D. T. Hickman, P. A. Lovatt and R. D. Peacock, *Chem. Commun.*, 1996, 1817.
29 C. Flassbeck, K. Wieghardt, E. Bill, C. Butzlaff, A. X. Trautwein, B. Nuber and J. Weiss, *Inorg. Chem.*, 1992, **31**, 21.
30 E. E. Lim and H. W. Wyckoff, *J. Mol. Biol.*, 1991, **218**, 449.
31 S. J. Brudenell, Ph.D. Thesis, Monash University, 1998.

Paper 8/09946D